sustainability

MDPI

Article

Comparative Analysis of MCDI and Circulation-MCDI Performance Under Symmetric and Asymmetric Cycle Modes at Pilot Scale

Changseog Oh [1], Hyun Je Oh [1,*], Seungjae Yeon [1], Bokjin Lee [1] and Jusuk An [1,2,*]

[1] Department of Environmental Research, Korea Institute of Civil Engineering and Building Technology (KICT), Goyang 10223, Republic of Korea; csoh@kict.re.kr (C.O.); yeon@kict.re.kr (S.Y.); bokjinlee@kict.re.kr (B.L.)
[2] Department of Civil and Environmental Engineering, Yonsei University, Seoul 03722, Republic of Korea
* Correspondence: hjoh@kict.re.kr (H.J.O.); jusuk@kict.re.kr (J.A.)

Abstract

This study compares the operational performance of membrane capacitive deionization (MCDI) and circulation-MCDI (C-MCDI) under symmetric (2/2, 3/3, 4/4 min) and asymmetric (5/2, 5/3, 5/4 min) adsorption/desorption cycles to identify efficient operating conditions at the pilot scale. A pilot system was tested with a NaCl solution of about 1000 mg/L, and 15 consecutive cycles were conducted to evaluate removal efficiency, specific energy consumption (SEC), and stability. MCDI consistently achieved over 90% removal efficiency with SEC below 0.6 kWh/m^3 across all modes, maintaining stable performance over 15 cycles. The 2/2 condition provided the shortest cycle time and the highest treated water productivity, making it the most efficient condition for the pilot-scale MCDI tested. C-MCDI showed stronger dependence on operating conditions, with the number of stable cycles ranging from 3 to 7 depending on desorption duration. Nevertheless, the 5/2 condition achieved about 91% removal efficiency with 0.58 kWh/m^3 SEC, and its extended adsorption period yielded about 2.5 times more treated water per cycle than the 2/2 case. Overall, this work provides a comparative pilot-scale evaluation of MCDI and C-MCDI, highlighting their advantages, limitations, and potential applications, and offering practical insights for energy-efficient and sustainable desalination strategies.

Keywords: circulation-membrane capacitive deionization; cycle stability; energy consumption; pilot-scale system; water recovery

check for updates

Academic Editor: Agostina Chiavola

Received: 15 September 2025
Revised: 22 October 2025
Accepted: 30 October 2025
Published: 31 October 2025

Citation: Oh, C.; Oh, H.J.; Yeon, S.; Lee, B.; An, J. Comparative Analysis of MCDI and Circulation-MCDI Performance Under Symmetric and Asymmetric Cycle Modes at Pilot Scale. *Sustainability* **2025**, *17*, 9744. https://doi.org/10.3390/su17219744

Copyright: © 2025 by the authors. Licensee MDPI, Basel, Switzerland. This article is an open access article distributed under the terms and conditions of the Creative Commons Attribution (CC BY) license (https://creativecommons.org/licenses/by/4.0/).

1. Introduction

With growing concerns over water scarcity caused by industrialization and population growth, seawater and brackish water have become essential alternative freshwater sources [1,2]. Conventional technologies, such as reverse osmosis (RO) and electrodialysis (ED), have been widely applied for this purpose [3]; however, they suffer from several limitations, including high energy consumption, membrane fouling, and the requirement for high-pressure operation [4,5].

Capacitive deionization (CDI) technology has attracted significant attention for overcoming these drawbacks [6,7]. CDI removes ions by electrically adsorbing them onto porous electrodes under low-voltage conditions [8]. It offers high energy efficiency and a simple system structure, making it suitable for treating low-to-moderate salinity water [9]. In particular, membrane capacitive deionization (MCDI), which incorporates ion-exchange

membranes into the CDI configuration, enhances ion selectivity and minimizes co-ion expulsion, significantly improving removal performance and pretreatment efficiency [10–12].

While MCDI addresses several limitations of conventional CDI, challenges related to water recovery and concentrate management still remain. Traditional MCDI processes typically use the same feed water during the adsorption and desorption stages, resulting in relatively low water recovery and limited reuse of the concentrate [13]. To address these limitations, a Circulation-MCDI (C-MCDI) process has been proposed, in which the concentrate is reused during the desorption stage [14,15]. This approach offers practical advantages such as increased water recovery, higher concentration, and reduced brine discharge [16]. However, empirical data on the long-term stability, energy efficiency, and removal performance of C-MCDI under repeated cycles are lacking [17]. Several recent studies have begun exploring pilot-scale MCDI systems under both symmetric and asymmetric modes [18–20], but side-by-side comparisons with C-MCDI remain rare.

Most previous studies have evaluated MCDI performance using symmetric cycle times (i.e., equal durations for adsorption and desorption) [21]. In contrast, systematic investigations into the effects of asymmetric timing on desalination performance and energy consumption are limited [22]. Furthermore, studies addressing the long-term cycle stability under various operating conditions and identifying the optimal operating parameters remain insufficient [23].

Therefore, this study provides a comparative pilot-scale evaluation of MCDI and C-MCDI under symmetric (2/2, 3/3, 4/4 min, referring to adsorption/desorption times in minutes) and asymmetric (5/2, 5/3, 5/4 min, referring to adsorption/desorption times in minutes) adsorption/desorption cycles [24,25]. Rather than claiming a universal optimal strategy, this work aims to identify efficient operating conditions for the tested pilot system, focusing on TDS removal efficiency, specific energy consumption, and cycle stability [26,27]. In addition, by linking the findings to energy-efficient desalination and reduced brine discharge, the study highlights the potential contribution of MCDI and C-MCDI to sustainable water resource management and environmentally responsible desalination practices.

2. Experimental

2.1. MCDI Module

The MCDI module used in this study (O2&B Co., Seoul, Republic of Korea) consisted of a stacked configuration of 231 porous carbon electrodes within a single unit, as schematically illustrated in Figure 1. Each circular electrode (200 mm diameter) was equipped with a cation exchange membrane (CEM) containing sulfonic acid functional groups on one side and an anion exchange membrane (AEM) containing quaternary ammonium functional groups on the other. A nylon spacer with a thickness of 180 μm is inserted between the ion exchange membranes to secure fluid flow paths. All components, including the electrodes, ion-exchange membranes, and spacers, had a central circular hole with a diameter of 25 mm, allowing the fluid to flow from the outer edge of the module toward the center. The feed water enters from the periphery of the module, flows radially inward through the spacers where electrosorption and desorption occur, and is then discharged through the central outlet. The module casing was made of a transparent acrylic material to allow visual observation of the internal fluid flow.

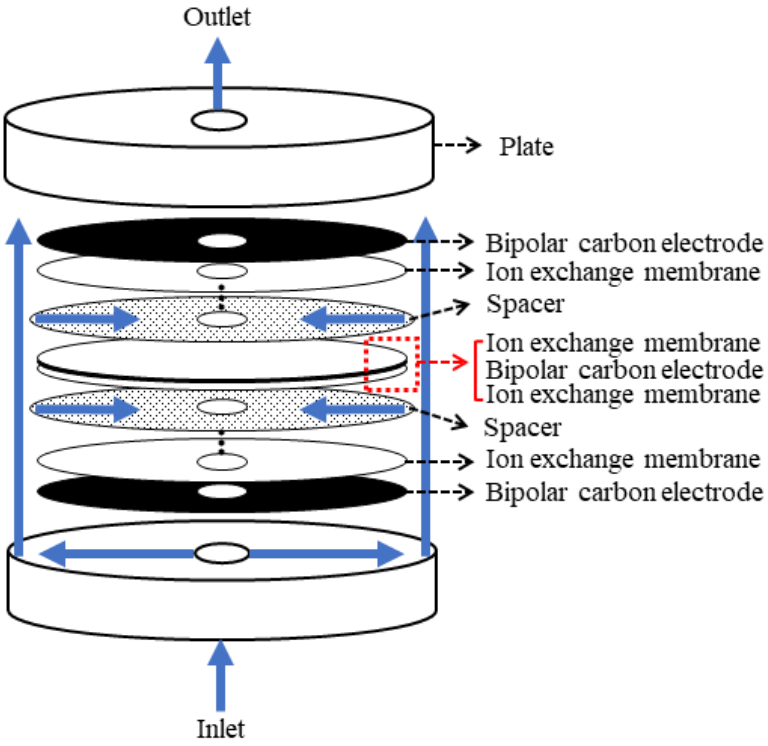


Figure 1. Schematic representation of the MCDI module configuration (The blue arrows indicate the water flow direction).

2.2. MCDI Pilot Unit and Operation Conditions

As shown in Figure 2, a pilot-scale MCDI unit was constructed for the experiment. The system consisted of a single MCDI module, a DC power supply, pumps for circulating feed water and concentrate, a concentrate storage tank, and a computer for system control and data acquisition. The raw water supply and treated water collection tanks were installed separately outside the pilot unit.

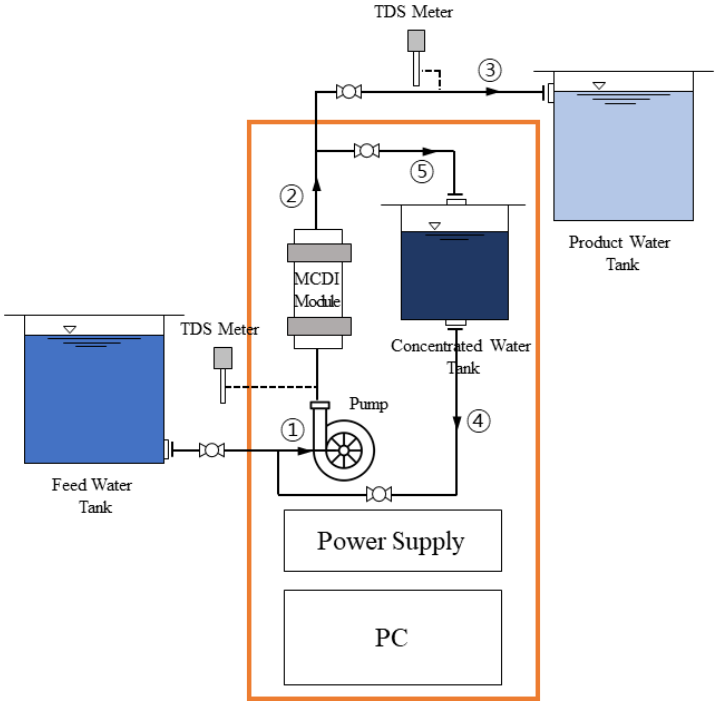


Figure 2. Schematic diagram of the MCDI pilot unit.

The feed solution was prepared by dissolving NaCl (99.5%, Samchun, Pyeongtaek, Republic of Korea) in tap water to achieve a total dissolved solids (TDS) concentration of approximately 1000 mg/L. The use of a synthetic NaCl solution was intended to standardize the operating conditions and ensure reproducibility of the results; however, this choice may limit direct applicability to natural brackish or industrial waters. The solution was supplied to the MCDI module at various flow rates using a centrifugal pump (HBI 4-30, Staris, Taiwan). In all experiments, the flow condition was maintained at 3 L/min for both MCDI and C-MCDI processes to ensure consistency. Although pH and temperature were not explicitly measured in this study, the experiments were conducted under ambient laboratory conditions, and it should be noted that these factors can influence ion adsorption and desorption behaviors in MCDI processes.

The system was operated in the constant voltage (CV) mode, with electrical power supplied by a DC power source (SJ-1260AN, SENICS, Cheonan-si, Republic of Korea). To prevent electrolysis within individual cells, the voltage per cell was limited to 1.2 V. Given that the module contained 231 bipolar electrode pairs, the total applied voltage was set to approximately 283 V. Additionally, to comply with the maximum output current rating of the power supply, the system current was restricted to below 20 A. During the operation, the actual current varied depending on the ion concentration in the feed solution.

The TDS concentrations of the treated water and concentrate were measured in real time at 1-s intervals using TDS sensors (3-2822-1 electrode, GF Signet, Irwindale, CA, USA). The sensors were calibrated before each set of experiments using standard NaCl solutions according to the manufacturer's protocol, and measurements were performed only after calibration was confirmed. To ensure reproducibility, each experiment was repeated three times under the same operating conditions, and while standard deviations were not explicitly calculated, the results of replicate runs showed negligible variations, and thus representative average values are presented. All the measurement data were automatically recorded and stored on a computer (17Z990-VA50K, LG Electronics, Seoul, Republic of Korea).

2.3. MCDI & Circulation MCDI Process

The MCDI and C-MCDI processes employed in this study consist of two sequential steps: adsorption and desorption, as illustrated in Figure 3. In these processes, voltage is applied periodically to induce the electrosorption and desorption of ions, resulting in treated water.

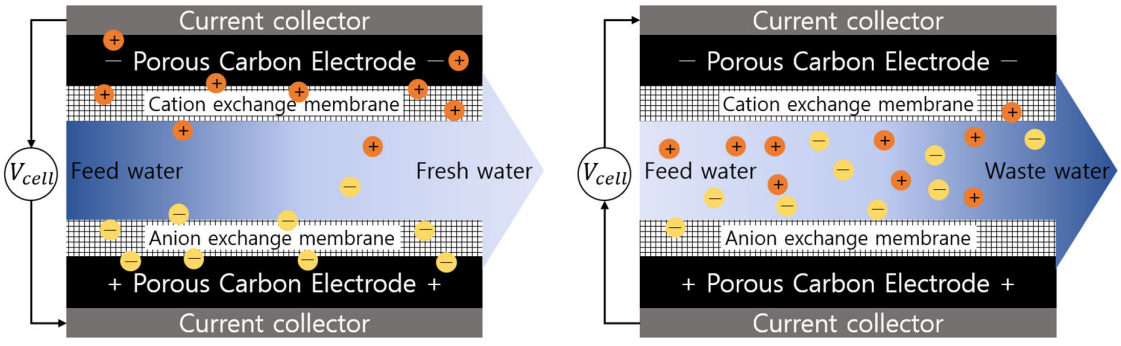


Figure 3. Adsorption (**left**) and desorption (**right**) processes in MCDI.

In the MCDI process, a positive voltage is applied during adsorption to induce ion removal via electrosorption onto the electrodes. In contrast, a negative voltage is applied during desorption to release the adsorbed ions. The same feed solution (NaCl with TDS of approximately 1000 mg/L) is used in adsorption and desorption. Water flows through

the system in the direction of inlet (1) → module (2) → product water outlet (3), as shown in Table 1.

Table 1. Experimental conditions of the MCDI and C-MCDI process experiment.

	Experimental Process	Water Flow	Feed Water (mg/L)	Applied Voltage (V)
MCDI Process	Adsorption	①→②→③	1000 (NaCl)	+283.2
	Desorption	①→②→③	1000 (NaCl)	−283.2
C-MCDI Process	Adsorption	①→②→③	1000 (NaCl)	+283.2
	Desorption	④→①→②→⑤	120 (Tap water)	−283.2

By contrast, the C-MCDI process utilizes a recirculated concentrated solution instead of raw water during the desorption step, a key distinguishing feature of this configuration. While the same 1000 mg/L NaCl solution is used during the adsorption step, the desorption step employs a stored concentrate solution with a TDS of approximately 120 mg/L, sourced from the concentrate tank. This solution is recirculated in the direction of (4) → (1) → (2) → (5), allowing for effective ion concentration and minimizing freshwater usage during regeneration. Consequently, the overall water recovery, defined as the ratio of product water to feed water, improved during the C-MCDI process [16].

Table 1 summarizes the system configurations and operating conditions for both processes, and Table 2 presents the experimental designs for various time conditions [15]. Adsorption and desorption times were changed independently between 2 and 5 min, allowing for symmetric (equal adsorption/desorption duration) and asymmetric (longer adsorption and shorter desorption) cycle configurations. A 5/5 condition was not included because excessively long symmetric cycles reduce experimental practicality and energy efficiency in pilot-scale operation, as highlighted in previous studies [16]. Through these tests, the effects of cycle timing on the conductivity variation, ion removal efficiency, and energy consumption were comparatively analyzed.

Table 2. Experimental design for MCDI and C-MCDI process under various adsorption/desorption time conditions.

Type of Cycle	Operation Conditions (Adsorption/Desorption, min)
Symmetric conditions	2/2, 3/3, 4/4
Asymmetric conditions	5/2, 5/3, 5/4

2.4. Data Analysis

The performances of the MCDI and C-MCDI processes were evaluated using three key parameters: TDS removal efficiency, specific energy consumption, and cycle stability. These metrics were calculated as follows:

The TDS removal efficiency was calculated using Equation (1):

$$\text{TDS removal efficiency } (\%) = \frac{C_o - C}{C_o} * 100 \quad (1)$$

where and are the TDS concentrations (mg/L) of the feed and product water, respectively.

The specific energy consumption (SEC) was calculated using Equation (2):

$$\text{Specific energy consumption } (\text{kWh/m}^3) = \frac{P * t}{V} \quad (2)$$

where is the average power (kW) during operation, is the duration of the adsorption or desorption step (h), and is the volume of treated water (m^3).

The cycle stability was defined as the number of continuous cycles in which both performance criteria—TDS removal efficiency $\geq$ 90% and energy consumption $\leq$ 0.6 kWh/m^3—were simultaneously satisfied. These thresholds were selected based on commonly reported benchmarks in CDI/MCDI studies, where 90% removal efficiency is generally considered sufficient for practical desalination applications, and an SEC below 0.6 kWh/m^3 has been suggested as a representative value for energy-efficient operation at the pilot scale [28]. Accordingly, these criteria provide a reasonable and practical basis for comparing the stability of different operating modes.

3. Results and Discussion

3.1. Variations in Electrical Conductivity According to Adsorption/Desorption Time

Figures 4 and 5 show the variations in the conductivity ratio (C/C_0) under different adsorption/desorption time conditions for the MCDI and C-MCDI processes, respectively. Under all conditions, a typical cyclic pattern was observed, characterized by a sharp decrease in C/C_0 during adsorption and a sharp increase during desorption. This behavior corresponds to ion removal and release through electrosorption and electrodesorption mechanisms.

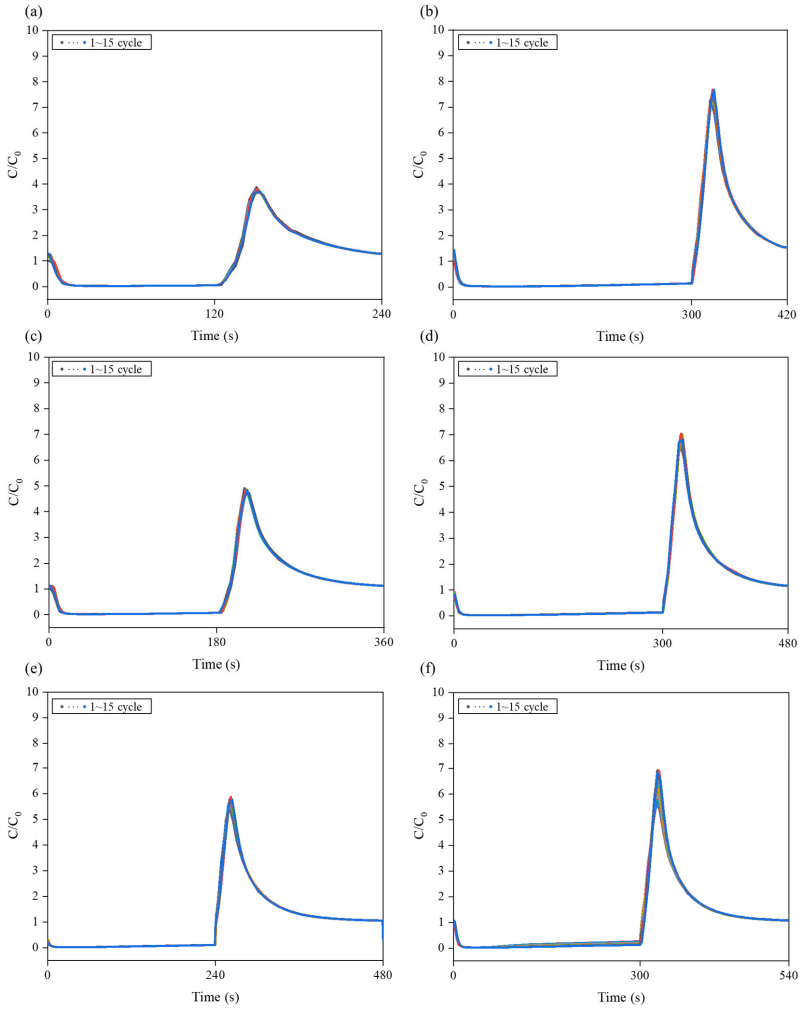


Figure 4. Variations in normalized conductivity (C/C_0) in the MCDI process under symmetric conditions: (**a**) 2/2 min, (**c**) 3/3 min, (**e**) 4/4 min, and asymmetric conditions: (**b**) 5/2 min, (**d**) 5/3 min, (**f**) 5/4 min.

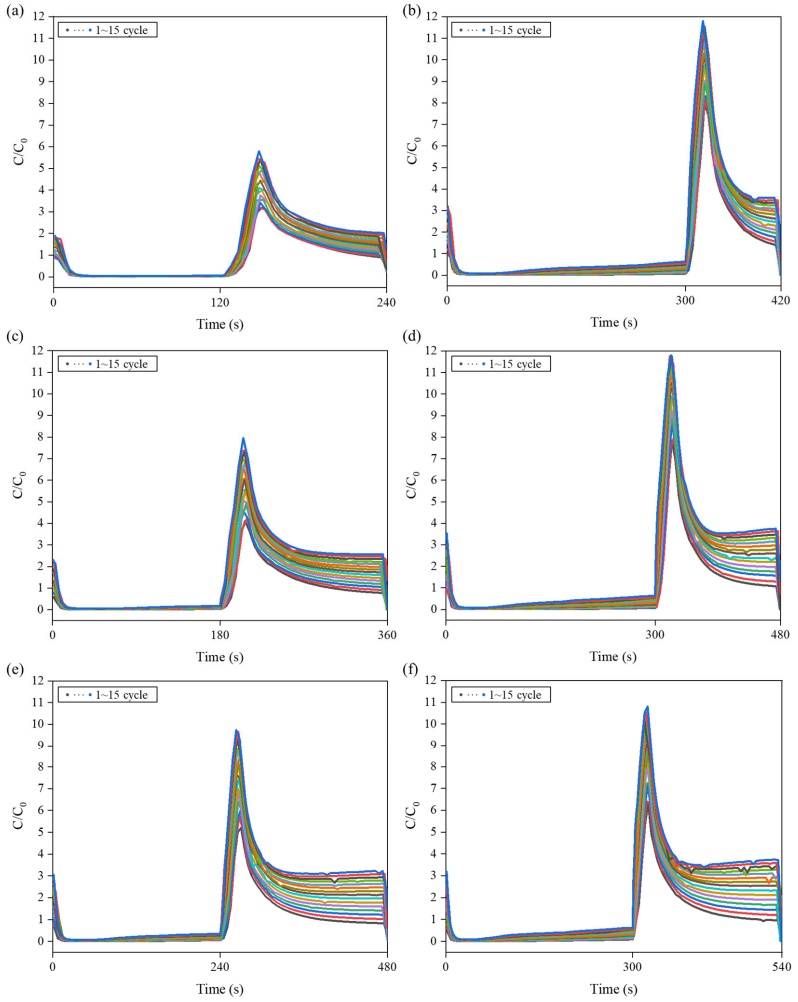


Figure 5. Variations in normalized conductivity (C/C_0) in the C-MCDI process under symmetric conditions: (**a**) 2/2 min, (**c**) 3/3 min, (**e**) 4/4 min, and asymmetric conditions: (**b**) 5/2 min, (**d**) 5/3 min, (**f**) 5/4 min.

In the MCDI process (Figure 4), the conductivity behavior under symmetric conditions (2/2, 3/3, and 4/4) showed that the C/C_0 peak during desorption gradually increased from approximately 4 to 6 as the cycle time increased; this indicated that more ions were adsorbed during more extended adsorption periods, resulting in higher concentrations during desorption. In contrast, under asymmetric conditions (5/2, 5/3, and 5/4), the C/C_0 peak during desorption remained relatively constant regardless of desorption duration, suggesting that the effect of desorption time was limited or that the desorption process was approaching saturation. Furthermore, the C/C_0 value at the end of the desorption step was higher than 1 when the desorption time was short, but approached 1 as the desorption time increased; this implies that insufficient desorption over short durations resulted in residual ions remaining in the module. These results suggest that the desorption time directly affects ion recovery in MCDI and increasing the desorption time under symmetric conditions can lead to improved performance.

In the case of the C-MCDI process (Figure 5), the conductivity behavior during the desorption step exhibited noticeable concentration variations depending on the adsorption/desorption duration. Under symmetric conditions (2/2, 3/3, and 4/4), the C/C_0 peak during desorption increased with longer desorption times, reaching approximately 6 for 2/2 and up to 10 for 4/4; this indicates that longer desorption durations lead to a greater release of concentrated ions, intensifying ion accumulation in the concentrate tank.

Under asymmetric conditions (5/2, 5/3, and 5/4), similar patterns were observed, where high desorption peaks were maintained in the initial cycles but gradually increased over repeated cycles. This trend implies that the concentrated discharge during desorption continued to accumulate over time, and the shorter the desorption time, the more significant the accumulation of unreleased ions. Ultimately, owing to the high water recovery of the C-MCDI system, a gradual increase in the desorption peaks was inevitable, emphasizing the necessity of securing an adequate desorption time to maintain system performance.

3.2. Removal Efficiency and Energy Consumption Under Symmetric Conditions

Figure 6 compares the changes in TDS removal efficiency and specific energy consumption for the MCDI and C-MCDI processes under symmetric operating conditions (2/2, 3/3, and 4/4). As shown in Figure 6a,b, the MCDI process maintained a stable removal efficiency of over 90% throughout all the cycles, with minimal variation across different time conditions. In contrast, the C-MCDI process exhibited an initial removal efficiency of more than 90%; however, a gradual decline was observed over repeated cycles. Notably, under the 4/4 condition, the efficiency decreases to below 70% after 15 cycles. This trend is attributed to ion accumulation between the electrodes and membranes in the C-MCDI configuration, which negatively affects long-term removal performance.

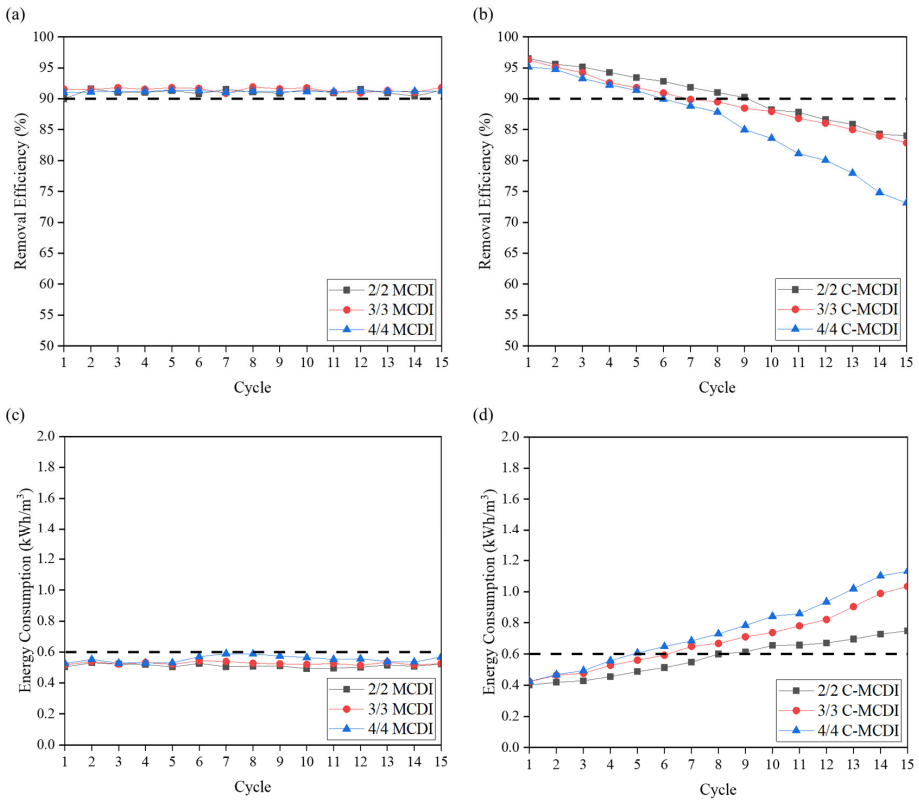


Figure 6. Comparison of removal efficiency and specific energy consumption of the MCDI and C-MCDI processes under symmetric adsorption/desorption conditions (2/2, 3/3, and 4/4): (**a**) MCDI removal efficiency, (**b**) C-MCDI removal efficiency, (**c**) MCDI specific energy consumption, (**d**) C-MCDI specific energy consumption.

Regarding energy consumption (Figure 6c,d), the MCDI process consistently maintained low consumption levels below 0.5 kWh/m^3, with negligible differences among the tested time conditions. On the other hand, the C-MCDI process showed a similar energy consumption as MCDI in the initial cycles, but it gradually increased with repeated operations. Under the 4/4 condition, the specific energy consumption rose to approxi-

mately 1.4 kWh/m^3 in the final cycle. This increase was likely due to the additional energy required to desorb the accumulated ions.

These results suggest that, while the MCDI process offers advantages in terms of stable removal efficiency and low energy consumption, the C-MCDI process is more sensitive to operational settings because of its structural characteristics. In particular, its performance is closely related to desorption efficiency and concentrate accumulation. Therefore, to fully leverage the benefits of C-MCDI, it is essential to determine the optimal conditions that minimize the performance degradation and energy increase. The analysis under asymmetric conditions in the following section provides further insight into this optimization.

3.3. Removal Efficiency and Energy Consumption Under Asymmetric Conditions

Figure 7 compares the TDS removal efficiencies and specific energy consumptions of the MCDI and C-MCDI processes under asymmetric adsorption/desorption time conditions (5/2, 5/3, and 5/4). As shown in Figure 7a,b, the MCDI process maintained a stable removal efficiency of approximately 90% under all conditions, with negligible differences according to the cycle time. This result demonstrates that the MCDI process, owing to its relatively simple electrosorption-based mechanism, is less sensitive to changes in operation time and can maintain consistent performance without degradation, even under repeated cycling [17,29].

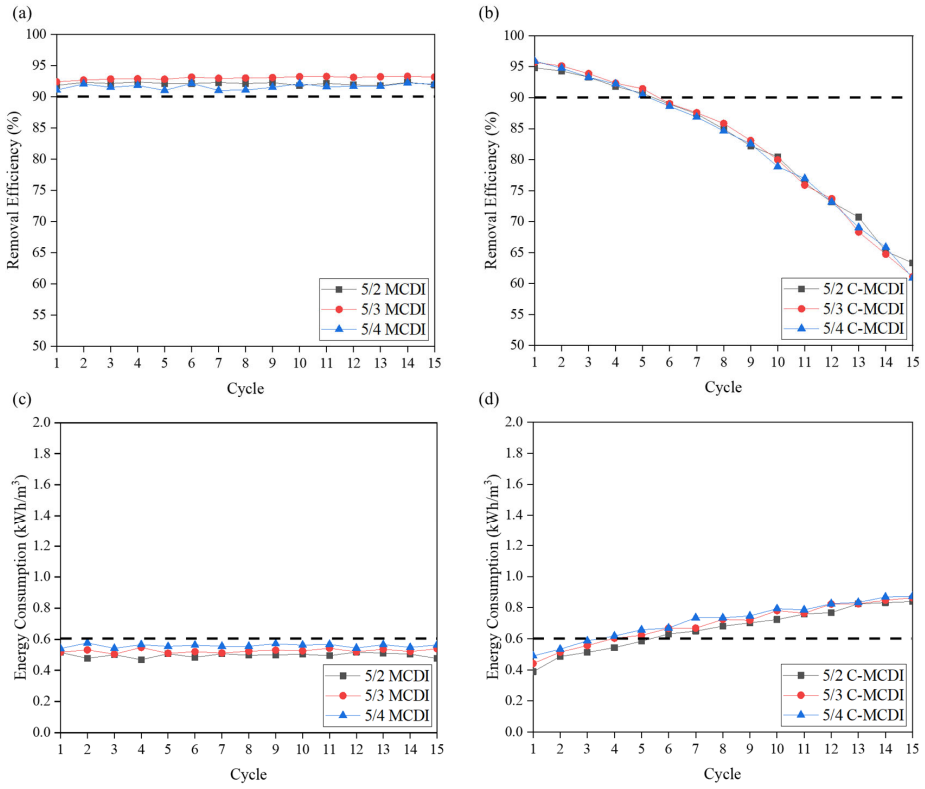


Figure 7. Comparison of removal efficiency and specific energy consumption of the MCDI and C-MCDI processes under asymmetric adsorption/desorption conditions (5/2, 5/3, and 5/4): (**a**) MCDI removal efficiency, (**b**) C-MCDI removal efficiency, (**c**) MCDI specific energy consumption, (**d**) C-MCDI specific energy consumption.

In contrast, the C-MCDI process showed a noticeable decline in removal efficiency as the desorption time decreased. In particular, under the 5/4 condition, the removal efficiency dropped to approximately 60% by the 15th cycle, and gradual efficiency degradation was observed under the 5/2 condition; this is attributed to the structural limitations of the C-MCDI configuration, in which a shorter desorption time relative to the adsorption time

leads to ion accumulation within the membrane stack, thereby reducing the regeneration efficiency over time. This phenomenon reflects the performance degradation caused by accumulation during repeated cycling, a key characteristic of C-MCDI systems.

Concerning energy consumption (Figure 7c,d), the MCDI process consistently maintained low consumption levels at approximately 0.5 kWh/m^3, showing minimal variation across operating conditions. In contrast, the C-MCDI process gradually increased energy consumption as cycling progressed, with the 5/4 condition exceeding 1.5 kWh/m^3, representing the highest value among all test cases; this was likely due to the increased energy required for insufficient desorption, where inadequate regeneration resulted in decreased energy efficiency.

These findings suggest that the MCDI process offers relatively stable operational characteristics under asymmetric conditions. In contrast, the C-MCDI process is more sensitive to operating parameters and can experience significant performance deterioration, particularly when desorption time is insufficient. Nevertheless, the C-MCDI process provides potential advantages, such as higher concentrate recovery and ion selectivity, making it a competitive alternative when properly optimized. Specifically, the ability of C-MCDI to recover highly concentrated brine compared with MCDI makes it more suitable for applications where high-value ion recovery or improved water recovery is required. Therefore, if the operational conditions are optimized to ensure sufficient desorption and low energy consumption, the C-MCDI process may be a viable and practical technology for field applications.

3.4. Determination of Optimal Operating Conditions

In this study, the optimal operating conditions for the MCDI and C-MCDI processes were determined based on three performance criteria: TDS removal efficiency ($\geq$90%), specific energy consumption ($\leq$0.6 kWh/m^3), and the maximum number of continuous cycles satisfying both. Table 3 summarizes each test condition's removal efficiency, energy consumption, and number of qualified cycles.

Table 3. Summary of removal efficiency, energy consumption, and feasible cycle count under various MCDI and C-MCDI processes operating conditions.

Conditions	Removal Efficiency (%)	Energy Consumption (kWh/m^3)	Feasible Cycle Count
2/2 MCDI	91.07	0.511	15
3/3 MCDI	91.48	0.526	15
4/4 MCDI	91.19	0.553	15
5/2 MCDI	92.08	0.497	15
5/3 MCDI	92.99	0.525	15
5/4 MCDI	91.63	0.558	15
2/2 C-MCDI	90.22	0.548	7
3/3 C-MCDI	90.93	0.592	6
4/4 C-MCDI	91.36	0.557	4
5/2 C-MCDI	90.72	0.584	5
5/3 C-MCDI	91.46	0.556	3
5/4 C-MCDI	90.47	0.587	3

For the MCDI process, all the tested conditions met the performance criteria. Among them, the 2/2 condition exhibited the shortest cycle time (4 min), while still achieving high removal efficiency (91.07%), low energy consumption (0.511 kWh/m^3), and stable operation for up to 15 cycles. Because of the structural characteristics of the MCDI process, in which adsorbed ions are expelled during desorption and the recovery ratios are relatively

low, the difference in the treated volume per cycle is minimal. As such, the number of cycles that can be completed per unit time becomes critical, and shorter cycles directly contribute to a higher overall throughput. Considering this, the 2/2 condition was identified as the optimal operating condition for the MCDI process, as it provided both stable performance and the highest treated water productivity per unit time.

For the C-MCDI process, all conditions (2/2, 3/3, 4/4, 5/2, 5/3, and 5/4) satisfied the set performance criteria. Notably, the 5/2 condition achieved high removal efficiency (90.72%) and low energy consumption (0.584 kWh/m^3), with stable performance over five cycles. In symmetric conditions (2/2, 3/3, 4/4), shorter adsorption/desorption times allowed more stable cycles, as frequent desorption reduced salt accumulation. In contrast, asymmetric conditions (5/2, 5/3, 5/4) showed fewer stable cycles when desorption was insufficient, as in the 5/3 case, where the relatively long adsorption time accelerated ion accumulation and performance decline.

The sharp contrast in cycle stability between the 2/2 (7 cycles) and 5/3 (3 cycles) conditions can be attributed to the imbalance between adsorption and desorption durations. In the 5/3 condition, the relatively long adsorption period accelerates ion accumulation within the electrodes, while the shorter desorption time is insufficient to fully regenerate the surface. This limitation is further amplified by the internal recirculation structure of the C-MCDI system, which promotes rapid salinity build-up in the concentrate channel. Consequently, ion desorption becomes progressively less effective, leading to a sharp decline in stable cycles compared with the more balanced 2/2 condition. This finding implies that in practical operation, C-MCDI systems may require design modifications such as improved regeneration protocols or extended desorption steps, as well as maintenance strategies to mitigate ion accumulation and preserve long-term performance.

Although the 2/2 condition supported up to seven cycles, the structural characteristics of the C-MCDI system, in which the concentrate was internally recirculated, allowed for a significant increase in treated water per cycle as the adsorption time increased. Given that the flow rate was fixed at 3 L/min, the treated volume per cycle is directly determined by the adsorption time. Because the desorbed concentrate was not discharged externally, the C-MCDI process enabled high recovery and improved ion accumulation efficiency. In this context, the 5/2 condition provides a practical balance between the cycle-level productivity and energy efficiency, making it the most favorable option.

These findings are consistent with previous studies that reported stable performance of MCDI under symmetric cycles but extended the understanding only to limited scales. In comparison, pilot-scale studies of brackish water desalination showed energy consumption values of approximately 0.8–1.0 kWh/m^3, which are higher than those obtained in this study [29]. Another study on brackish water application demonstrated successful CDI operation [20], but with lower cycle stability than observed in the present pilot-scale C-MCDI experiments. This comparison highlights the advantage of the present work in achieving both high removal efficiency and reduced SEC under realistic operating conditions.

Therefore, the 5/2 condition was identified as the optimal operating condition for the C-MCDI process because it simultaneously satisfied the performance criteria and maximized the treated volume per cycle. Given its high recovery and ion concentration capabilities, C-MCDI is expected to be a promising alternative for applications requiring efficient, selective ion recovery and high-water recovery rates. These findings indicate that the 2/2 MCDI mode can provide consistent and predictable performance for continuous operation in community-level water supply facilities, whereas the 5/2 C-MCDI mode may be more suitable for applications prioritizing high recovery or concentrated stream production, such as reuse of brine or recovery of specific salts.

4. Conclusions

This study systematically compared the performance of MCDI and C-MCDI processes under symmetric and asymmetric adsorption/desorption cycles at the pilot scale, highlighting both their strengths and limitations. MCDI consistently ensured stable operation with removal efficiency above 90% and SEC below 0.6 kWh/m^3, particularly under short cycle conditions (2/2), making it highly suitable for energy-efficient and reliable desalination. In contrast, C-MCDI demonstrated stronger dependence on operating time, but when optimized (e.g., 5/2), it achieved comparable efficiency while producing significantly higher water recovery and reduced brine discharge, which is advantageous for resource recovery applications. These findings provide practical insights for selecting between the two configurations depending on operational priorities—stability and energy efficiency for MCDI versus high recovery and concentrate reuse for C-MCDI. Beyond performance comparison, this work contributes empirical evidence for scaling CDI-based processes toward sustainable water management, and future studies should expand to real feedwaters and long-term operation to validate durability, cost-effectiveness, and system integration in practical settings.

Author Contributions: C.O.: formal analysis, investigation, and writing—original draft; H.J.O.: funding acquisition, and writing—review and editing; S.Y.: conceptualization, and writing—review and editing; B.L.: investigation, and writing—review and editing; J.A.: formal analysis, investigation, and writing—review and editing. All authors have read and agreed to the published version of the manuscript.

Funding: This work was supported by Korea Environment Industry & Technology Institute (KEITI) through the Project for developing innovative drinking water and wastewater technologies, funded by the Korea Ministry of Environment (MOE) (2020002700003) and the KICT Research Program (project no. 20250195-001, Development of low-energy/high-efficiency MCDI process and application to Malaysia) funded by the Ministry of Science and ICT.

Institutional Review Board Statement: Not applicable.

Informed Consent Statement: Not applicable.

Data Availability Statement: The original contributions presented in this study are included in the article. Further inquiries can be directed to the corresponding authors.

Conflicts of Interest: The authors declare no conflicts of interest.

References

1. Ruiz-García, A.; Nuez, I. Long-term intermittent operation of a full-scale BWRO desalination plant. *Desalination* **2020**, *489*, 114526. [CrossRef]
2. Porada, S.; Zhao, R.; Van Der Wal, A.; Presser, V.; Biesheuvel, P.M. Review on the science and technology of water desalination by capacitive deionization. *Prog. Mater. Sci.* **2013**, *58*, 1388–1442. [CrossRef]
3. Oddonetto, T.L.; Deemer, E.; Lugo, A.; Cappelle, M.; Xu, P.; Santiago, I.; Walker, W.S. Assessment of salt-free electrodialysis metathesis: A novel process for brine management in brackish water desalination using monovalent selective ion exchange membranes. *Desalination* **2024**, *592*, 118160. [CrossRef]
4. Wu, Q.; Liang, D.; Lu, S.; Wang, H.; Xiang, Y.; Aurbach, D.; Avraham, E.; Cohen, I. Advances and perspectives in integrated membrane capacitive deionization for water desalination. *Desalination* **2022**, *542*, 116043. [CrossRef]
5. Huang, Q.; Sheng, L.; Wu, T.; Huang, L.; Yan, J.; Li, M.; Chen, Z.; Zhang, H. Research progress on the application of carbon-based composites in capacitive deionization technology. *Desalination* **2025**, *593*, 118197. [CrossRef]
6. Sufiani, O.; Tanaka, H.; Teshima, K.; Machunda, R.L.; Jande, Y.A.C. Capacitive deionization: Capacitor and battery materials, applications and future prospects. *Desalination* **2024**, *587*, 117923. [CrossRef]
7. Tauk, M.; Folaranmi, G.; Cretin, M.; Bechelany, M.; Sistat, P.; Zhang, C.; Zaviska, F. Recent advances in capacitive deionization: A comprehensive review on electrode materials. *J. Environ. Chem. Eng.* **2023**, *11*, 111368. [CrossRef]

8. Suss, M.E.; Porada, S.; Sun, X.; Biesheuvel, P.M.; Yoon, J.; Presser, V. Water Desalination via capacitive deionization: What is it and what can we expect from it? *Energy Environ. Sci.* **2015**, *8*, 2296–2319. [CrossRef]
9. Hemmatifar, A.; Palko, J.W.; Stadermann, M.; Santiago, J.G. Energy breakdown in capacitive deionization. *Water Res.* **2016**, *104*, 303–311. [CrossRef]
10. Tang, W.; He, D.; Zhang, C.; Kovalsky, P.; Waite, T.D. Comparison of faradaic reactions in Capacitive Deionization (CDI) and Membrane Capacitive Deionization (MCDI) water treatment processes. *Water Res.* **2017**, *120*, 229–237. [CrossRef]
11. Yoon, H.; Jo, K.; Kim, K.J.; Yoon, J. Effects of characteristics of cation exchange membrane on desalination performance of membrane capacitive deionization. *Desalination* **2019**, *458*, 116–121. [CrossRef]
12. Biesheuvel, P.M.; Van Der Wal, A. Membrane capacitive deionization. *J. Membr. Sci.* **2010**, *346*, 256–262. [CrossRef]
13. Zhao, Y.; Wang, Y.; Wang, R.; Wu, Y.; Xu, S.; Wang, J. Performance comparison and energy consumption analysis of capacitive deionization and membrane capacitive deionization processes. *Desalination* **2013**, *324*, 127–133. [CrossRef]
14. Oh, C.; An, J.; Yeon, S.; Oh, H.J. Evaluation of total dissolved solids removal characteristics by recycling concentrated water in membrane capacitive deionization process. *Desalination Water Treat.* **2022**, *264*, 54–61. [CrossRef]
15. Oh, C.; Lee, B.; An, J.; Yeon, S.; Je Oh, H. Performance optimization of a pilot-scale Membrane Capacitive Deionization (MCDI) system operating with circulation process. *Sep. Purif. Technol.* **2024**, *343*, 126937. [CrossRef]
16. Lee, B.; Oh, C.; An, J.; Yeon, S.; Oh, H.J. Optimizing operational conditions of pilot-scale membrane capacitive deionization system. *Sustainability* **2023**, *15*, 16809. [CrossRef]
17. Chen, T.-H.; Kao, Y.-H.; Shen, Y.-Y.; Fan, C.-S.; Hou, C.-H. Pilot-scale membrane capacitive deionization for water reclamation: Commissioning, performance benchmarking, and long-term assessment. *Desalination* **2025**, *599*, 118428. [CrossRef]
18. Yoon, H.; Jeon, S.; Min, T.; Lee, C.K.; Lee, G. Pilot-scale capacitive deionization for water softening: Performance, energy consumption, and ion selectivity. *J. Environ. Chem. Eng.* **2024**, *12*, 114259. [CrossRef]
19. Alotaibi, Z.S.; Alharbi, K.N.; Alharbi, Y.; Almoiqli, M.S. Innovative pilot plant capacitive deionization for desalination brackish water. *Appl. Water Sci.* **2024**, *14*, 26. [CrossRef]
20. Nordstrand, J.; Dutta, J. Flexible modeling and control of capacitive-deionization processes through a linear state-space dynamic Langmuir model. *npj Clean Water* **2021**, *4*, 5. [CrossRef]
21. Ramachandran, A.; Oyarzun, D.I.; Hawks, S.A.; Stadermann, M.; Santiago, J.G. High water recovery and improved thermo dynamic efficiency for capacitive deionization using variable flowrate operation. *Water Res.* **2019**, *155*, 76–85. [CrossRef]
22. Kim, N.; Lee, J.; Hong, S.P.; Lee, C.; Kim, C.; Yoon, J. Performance analysis of the multi-channel membrane capacitive de ionization with porous carbon electrode stacks. *Desalination* **2020**, *479*, 114315. [CrossRef]
23. Zhao, R.; Biesheuvel, P.; Miedema, H.; Bruning, H.; Van der Wal, A. Charge efficiency: A functional tool to probe the doublelayer structure inside of porous electrodes and application in the modeling of capacitive deionization. *J. Phys. Chem. Lett.* **2010**, *1*, 205–210. [CrossRef]
24. Hassanvand, A.; Chen, G.Q.; Webley, P.A.; Kentish, S.E. A Comparison of multicomponent electrosorption in capacitive de ionization and membrane capacitive deionization. *Water Res.* **2018**, *131*, 100–109. [CrossRef] [PubMed]
25. Gao, X.; Omosebi, A.; Landon, J.; Liu, K. Enhanced salt removal in an inverted capacitive deionization cell using amine modified microporous carbon cathodes. *Environ. Sci. Technol.* **2015**, *49*, 10920–10926. [CrossRef] [PubMed]
26. Dorji, P.; Kim, D.I.; Hong, S.; Phuntsho, S.; Shon, H.K. Pilot-scale membrane capacitive deionisation for effective bromide removal and high water recovery in seawater desalination. *Desalination* **2020**, *479*, 114309. [CrossRef]
27. Xing, W.; Liang, J.; Tang, W.; He, D.; Yan, M.; Wang, X.; Luo, Y.; Tang, N.; Huang, M. Versatile applications of Capacitive Deionization (CDI)-based technologies. *Desalination* **2020**, *482*, 114390. [CrossRef]
28. Tan, C.; He, C.; Fletcher, J.; Waite, T.D. Energy recovery in pilot scale membrane CDI treatment of brackish waters. *Water Res.* **2020**, *168*, 115146. [CrossRef]
29. Liu, H.-C.; Lee, M.; Hou, C.-H. Development and environmental performance of a pilot-scale membrane capacitive deionization system for wastewater reclamation: Long-term operation and life cycle analysis. *Sci. Total Environ.* **2024**, *957*, 177454. [CrossRef]

Disclaimer/Publisher's Note: The statements, opinions and data contained in all publications are solely those of the individual author(s) and contributor(s) and not of MDPI and/or the editor(s). MDPI and/or the editor(s) disclaim responsibility for any injury to people or property resulting from any ideas, methods, instructions or products referred to in the content.